ISSN: 1343-4292
Volume 140, Issue 07, October, 2022

Cytotoxicity of New Complexes of Platin and Copper with New Ligand Synthesized by Mannich Reaction

Mosa Jaafar Mosa[1*], Rehab Al-Hassani[2], Fatin Fadhel Alkazazz[2]

Alsafwa university college Department. of Nursing, Iraq[1]
Mustansiriyah University College of Science Department of Chemistry, Iraq[2]

Corresponding author: 1*

ABSTRACT— New ligand was synthesized as Mannich base containing 1,3,4-Oxadiaole ring and characterized by FT-IR,UV, Elemental analysis, ^{1}HNMR and ^{13}CNMR. Then a complexes of Pt^{+4} and Cu^{+2} were synthesized by complexation with prepared ligand and characterized by UV, FT-IR, flame atomic absorption Magnetic susceptibility and molar conductivity. The results approved success of synthesis procedure. The antibacterial activity and cytotoxicity assay were tested for the ligand and their metal complexes. The result show the complexes active compound as antibacterial and antifungal against bacterium *Escherichia coli*(gram negative) and *Staphylococcus aurous* (gram positive) also against fungi *Candida albicans* and *Aspergillus flavus*. Cytotoxicity tested on normal cell line (MDCK) and the results showed that LD50 of L = 936 µg/ml, toxicity of Pt = 875 µg/ml and toxicity of Cu = 1356 µg/ml. Toxicity also tested for the ligand and both complexes against Human lung cancer cell line, the results showed that LD50 of Pt complex = 615 µg/ml, toxicity of Cu complex = 653 µg/ml and toxicity of free ligand = 620 µg/ml. Low MIC was resulted for the ligand and both complexes compared with Amoxicillin and Ampicillin as antibiotic.

KEYWORDS: Cytotoxicity, Mannich Reaction, Ampicillin

1. INTRODUCTION

Mannich reaction is an organic reaction which consists of an amino alkylation of an acidic proton placed next to a carbonyl functional group with formaldehyde and ammonia or any primary or secondary amine [3]. The final product is a β-amino-carbonyl compound also known as a Mannich base [15]. As well as it is also used in the synthesis of important compounds in medicinal application e.g. rolitetracycline, fluoxetine, tramadol, and tolmetin, other applications are in agro chemicals such as plant growth regulators, paint- and polymer chemistry, catalysts and crosslinking [11].

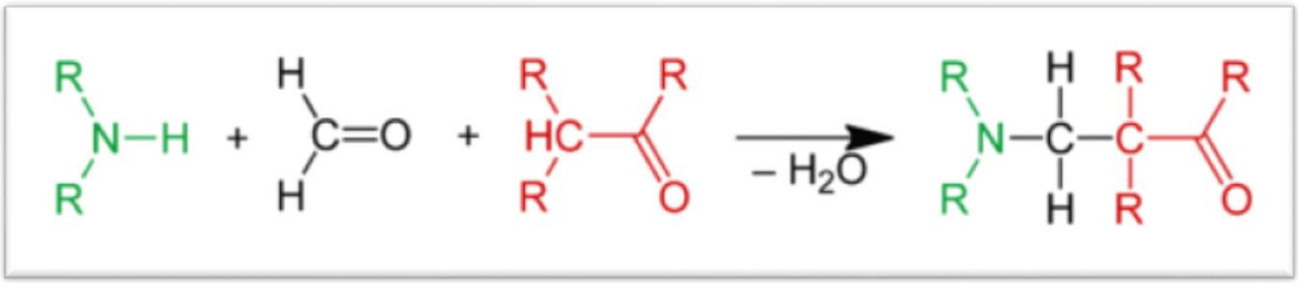

As ligands, many researcher used mannich reaction to synthesis their ligand and complexation with many transition metals [11]. Thione derivatives of Mannich base had spread rang in complex synthesizing due to

less basicity of sulfur than oxygen and easy donating of electron pair [1], as shown in example below:

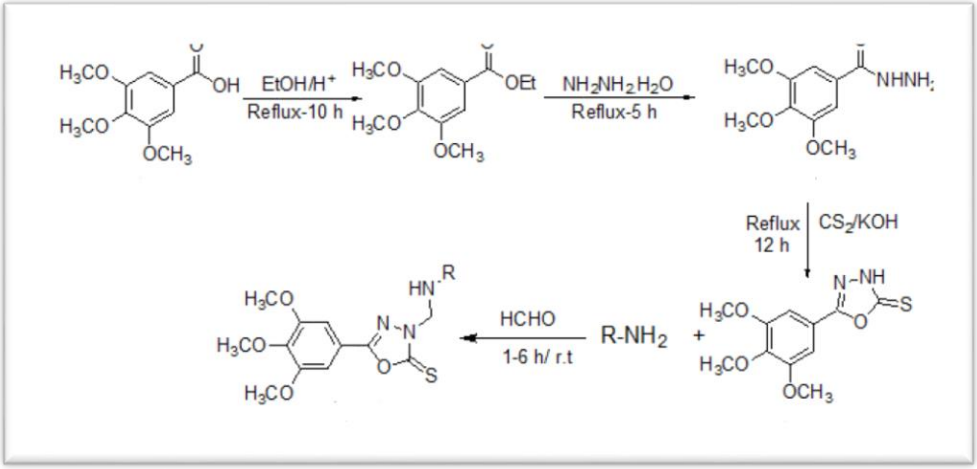

Synthesis of Mannich Bases derivedfrom 1, 3, 4-oxadiazole-2-thiones [2]

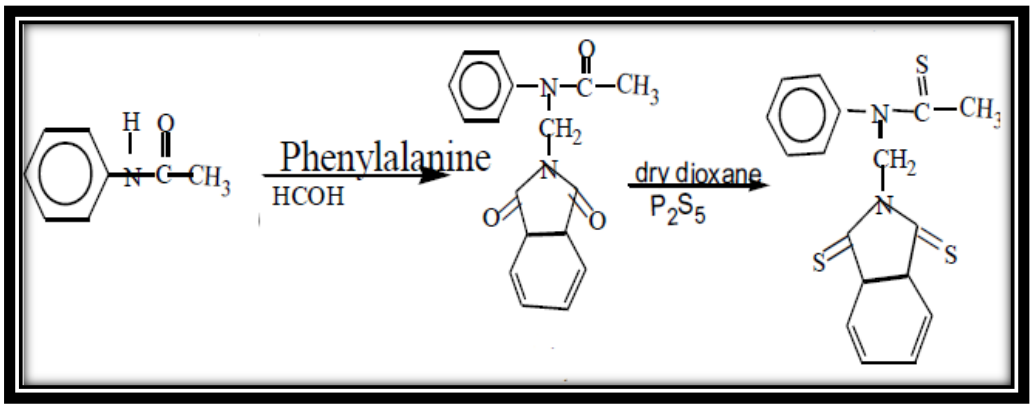

Synthesis of thione derivative of Mannich Bases by [4]

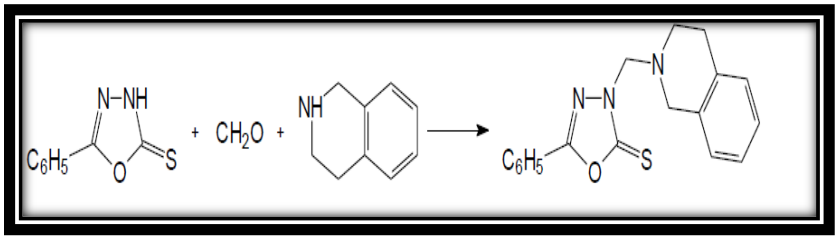

Preparation of Mannich base derived from 1,3,4-oxadiazole-2-thione [3]

ISSN: 1343-4292
Volume 140, Issue 07, October, 2022

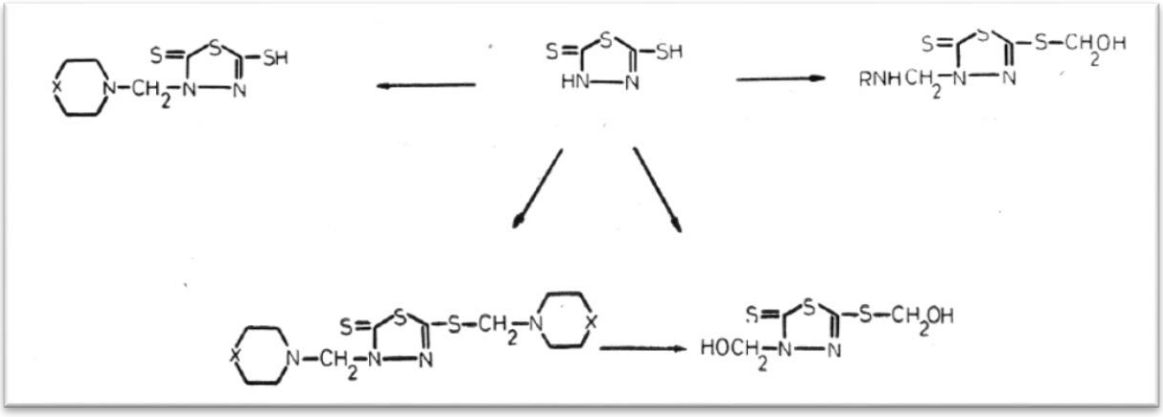

Preparation of Mannich base from 2,5-Dimercapto-1,3,4-thiadiazole [9].

In this study we trying to evaluate the *invitro* cytotoxicity of our compounds and test the anticancer activity for it, obviously our compounds were synthesized according Mannich reaction with thione derivatives for copper(II) and platin(IV).

2. Procedure

2.1 Materials

The reagents were obtained commercially and used without further purification.

2.2 Syntheses

2.2.1 General procedure for the synthesis of ligand

A 0.001 mole (0.214 g) of 6-Methoxy-2-naphthylacetic acid was mixed with 15 mL of Methanol and 10 drops of H2SO4 was added gradually to solution of. The mixture was refluxed at 60 oC for 4 h. An ester product precipitate was separated out and washed with acetone [1]. The ester product 0.001mole (0.22 g) was refluxed with hydrazine (10.5 mL) in presence of methanol and refluxed at 60 oC for 1.5 h. An amide product precipitate was separated out and washed with acetone [3]. The amide product0.001mole (0.22g) was refluxed with CS2 (7.5 mL) in presence of methanol and KOH and then refluxed at 70 oC for 2 h. A thiolate salt product precipitate was separated out and washed with acetone. 15drops of HCl was added slightly to salt to release the 1,3,4-Oxadiazole product (Pollak and Stanovnik, 1965). Last step and according Mannich reaction the ligand was synthesized by adding 5 mL of piprydine and 15 mL of formaldehyde to the solution of 0.001 mole 0.28 g from 1,3,4 Oxadiazole in methanol, the mixture was refluxed at 75 oC for 3 h. A precipitate was separated out and washed with acetone and dried at room temperature [15].

2.2.2 General procedure for the synthesis of platin (IV) and copper(II)-complexes

The complexes were prepared as shown in study (Zheng et al., 2014) by the addition of heated solution of the metals salt, 0.001mole (0.225 g) of CuCl2.5H2O and 0.0005mole (0.187 g) PtCl4.2H2O in appropriate amount of Methanol [10mL]to the stirred and heated solution [65 °C] of the 1,3,4Oxadiazole 0.001 mole (0.37 g) previously dissolved in the Methanol (Abdulameer, Abbas and Mosa, 2019.

2.3 characterization

The melting points of all synthesized compounds were determined on electro thermal capillary apparatus, Coslab melting point, FT-IR spectra in the range (4000-600) cm-1.were.recorded using FT-IR.8400S

Shimadzu Spectrophotometer, UV-Visible spectra were measured using Shimadzu UV-Vis. 160 Ultra-Violet Spectrophotometer in the range [200-1000 nm], using chloroform as a solvent(10-3 M) at 25 ºC using quartz cell of 1.0 cm length, Electrical conductivity measurements were carried out using WTW conductivity meter, with using DMF solutions at 25 ºC as a solvent ($1*10^{-3}$M), The magnetic susceptibility values of the prepared complexes were obtained at room temperature using Magnetic Susceptibility Balance - Sherwood Scientific Ltd(UK) at Chemistry department / College of Science /Al-Mustansiriyah University. ^{1}H, ^{13}C -NMR spectra, ligands and diamagnetic complexes were acquired using 1H, 13C -NMR spectra were measured on a BRUKER AV 400 Avance-III (500 MHz and 125 MHz) instrument in d6 DMSO solution with theTMS as internal standard. The samples were recorded of the National Institute of Technology, Tahran, Iran. Elemental CHNS analyses for ligands and their metal ion complexes were carried out on a Fison EA 1108 analyzer AL - Albait University, Amman, Jordan. The flame atomic absorption measurements was used to determine the metal contents by using Nova350 Spectrophotometer, in Ibn Sina State Company.

2.4 In vitro determination the cytotoxicity study

2.4.1 Preparation of drug solutions

Each one of the complexes and ligand were dissolved in 10 % dimethylsulfoxide (DMSO) in distilled water. These stock solutions were diluted before use in culture medium containing fetal bovine serum FBS, RPMI media and antibiotic. MTT 3-(4,5- dimethylthiazol-2-yl)-2,5-diphenyl-tetrazolium-bromide was dissolved in a phosphate buffer saline having a pH of 7.2, and then filtered.

2.4.2 Cell culture

The MDCK cell lines were provided by Tissue Culture Laboratory in the College of Medicine / University of Babylon. The cells were supplemented with 10 % fetal bovine serum (FBS, Sigma Aldrich, Munich, Germany), penicillin (100 IU/mL), streptomycin (100 µg/mL) in a humidified atmosphere of 95 % air/5 % CO_2 at 37 °C. and washed three times in serum- free PBS. The number of viable cells was determined by trypan blue exclusion.

2.4.3 Cytotoxicity assay

The effects of the tested compounds on cell viability were determined using MTT colorimetric technique. MDCK cells placed in individual wells in 96-multiplates. The next day the medium was exchanged with 100 µL of our different compounds, which had been serially diluted 2-fold in the medium to concentrations ranging from 1000 µg to 31.5 µg in growth medium. Each compound was tested in four times. The cells were incubated at 37 °C for 24 h. After incubation the supernatant was removed and 15 % MTT solution 5 mg/mL in PBS, 10 µL medium was added to each well. After an additional 4 h of incubation at 37 °C, the medium with MTT was removed and DMSO (150 µL) with Trypan blue solution buffer (20 µL) was added to dissolve the crystals. The plates were shaken for 10 min. The optical density of each well was determined at 595nm using ELISA Reader [6].

The percentage of cytotoxicity was calculated using the formula:

$$\% \text{ viability} = (AT - AB) / (AC - AB) \times 100\%$$

Where, AT = Absorbance of treated cells (with complex).

AB = Absorbance of blank (only medium).

AC = Absorbance of control (untreated).

$$\% \text{ Inhibition} = 100 - \% \text{ viability}$$

Each of the tested complexes was evaluated for cytotoxicity in four separate experiments.

ISSN: 1343-4292
Volume 140, Issue 07, October, 2022

2.5 Biological activity

2.5.1 Antibacterial activity

Two *in vitro* techniques were procceded for studying antibacterial activity against the (*Escherichia coli* and *Staphylococcus aureus*) and *Candida (Aspergillusflaveus , albicans)*, DMSO was used as a solvent and as a control, for both techniques, the concentrations of the compounds in the solvent were 10^{-3}M. The first technique was the Disc Sensitivity Test this method involves the exposure of the zone of inhibition toward the diffusion of micro-organism on agar plate. The plates were incubated for 24hr. at 37^0C, the zone of inhibition of bacterial growth around the disc was observed. The second technique was to obtain the sensitivity of each micro-organism toward the new metal complexes by determining the minimal inhibitory concentration (MIC) which was gained by using Tube Dilution Method. The (MIC) of the new ligands and their metal complexes for each micro-organism was measured at the lowest concentration of the compound required to inhibit the growth of these micro-organisms, these tubes containing different concentrations of the new ligands and its metal complexes were incubated at 37^0C for 45hr. Furthermore, two of know antibiotics(Ampicillin and Amoxicillin), were taken as standard to compare their activity with those of the new ligands and their metal complexes, these antibiotics cover a wide range of structural pharmacological moieties [12].

2.5.2 Antifungal activity

In order to complete this study, the new ligand and their metal complexes were tested for their *invitro* growth inhibitory activity against a pathogenic fungus, i.e. *Aspergillusflaveus and Candida albicans*. on Potato dextrose agar medium and incubated at 300C for 72hr., DMSO was used as a solvent and as a control, for both techniques, the constructions of the compounds in this solvent were 10^{-3}M. The inhibition of fungal growth, expressed in percentage terms, were determined on the growth in test plates compared to the respective control plates, as given by the Vincent equation.

$$\text{Inhibition\%}=100(C-T) / C$$

Where: C=Diameter of fungal growth on the control plate.
T= Diameter of fungal growth on the test plate.

2.6 Hemolysis test

38 mL of ringer was mixed with 2 mL of blood in conical flask containing anticoagulant sodium citrate, the 2 mL of this solution added to 2 mL of complex and incubation at 37 0C for 30 min. the absorbance taken at 460 nm against Ringer solution as blank and the solution of ringer with blood used as control. The hemolysis calculated by equation [10].

$$\text{Hemolysis \%} = (A_{\text{sam.}} - A_{\text{blank}}) / (A_{\text{control}} - A_{\text{blank}}) \times 100$$

3. Results and discussion

3.1 Characterization of ligand and complex

Electronic spectra

The (U.V-Vis) absorption spectrum of ligand (L) in ethanol exhibited three absorption bands at (278 nm, 35971cm-1), (315 nm, 31746cm-1), were assigned to ($\pi\rightarrow\pi^*$), ($n\rightarrow\pi^*$) transitions, and one band as a shoulder at (350 nm, 28571 cm-1) showed in the figure 3.1 assigned to ($n\rightarrow\pi^*$) intra ligand transition [16].

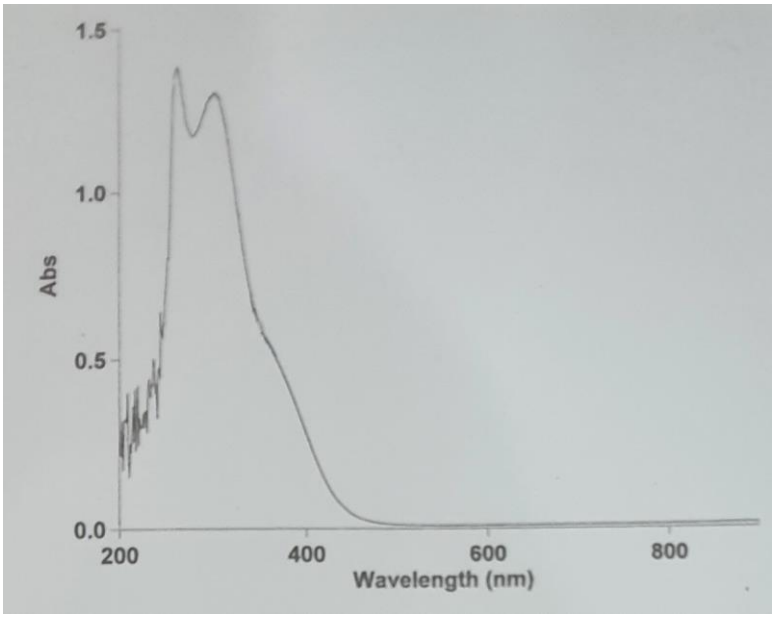

Fig3.1 UV spectrum for ligand

The spectrum of **LCu** complex in $CHCl_3$ shows one broadband at(690 nm, 14492cm^{-1})which agrees to $^2B_1g \rightarrow {}^2A_1g$ transition and two shoulder bands at [(432nm, 23148cm^{-1})and (399 nm, 25063cm^{-1}) allocated to $^2B_1g \rightarrow {}^2B_2g + {}^2Eg$ (ν_2) transitions [16] the position of these bands is approve with configuration square planer and it is shown in the scheme 3.1 and in a figure3.2. At room temperature the value of magnetic moment was found to be (1.82B.M), which approve with square planar geometry for Cu (II) complex**,** the conductivity in DMF mentions to the non-ionic showing for this complex. From the electronic spectra data, FT-IR spectroscopy data and flame atomic absorption, a square planar geometry around the Cu (II) ion can be proposed as shown in scheme 3.1.

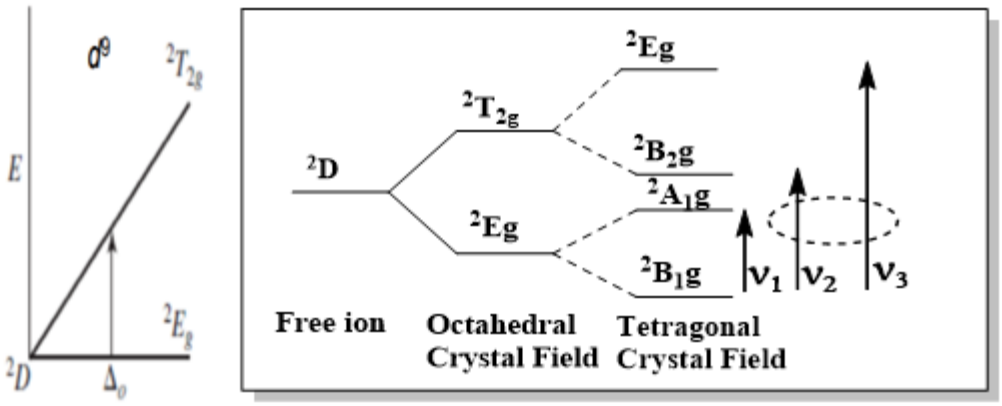

ISSN: 1343-4292
Volume 140, Issue 07, October, 2022

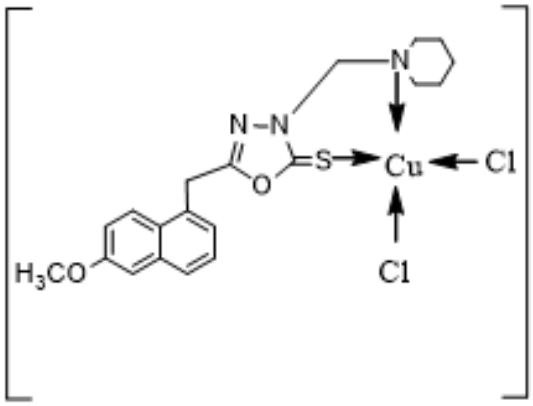

scheme 3.1: Geometry for CuL

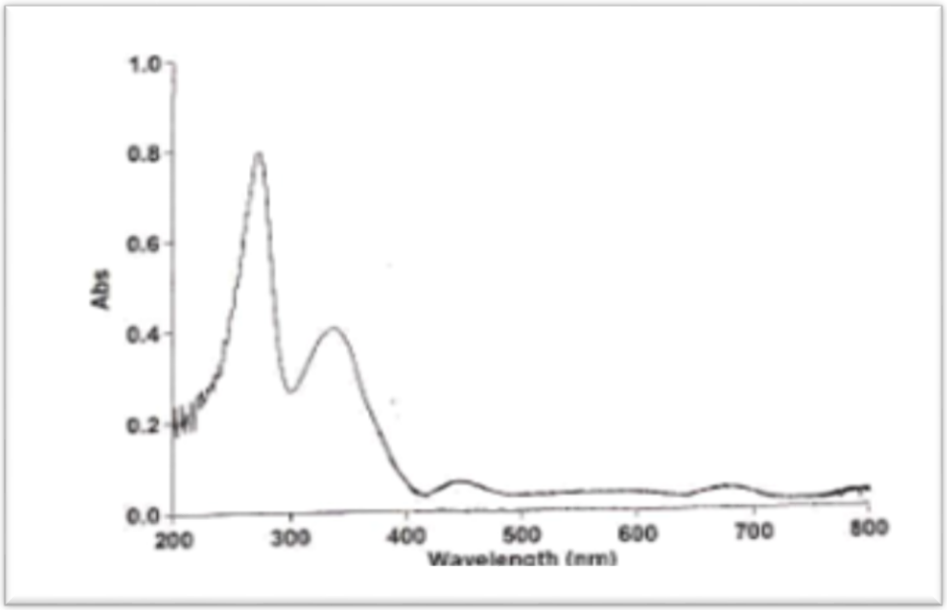

Fig 3.2 UV spectrum for Cu L

The (LPt) complex in chloroform exhibited weak. absorption bands at (508 nm, 19685cm-1), the second and third as more intense bands at(438nm, 22831 cm-1) and (399nm, 30303 cm-1) respectively figure3.3 these three bands could simply be due to the transitions 1A1g→3T1g, 1A1g→3T2g and (L→Pt Charge Transfer) respectively [8]. The magnetic moment of the present complex is (0.05 B.M) of the present Pt(IV) complex (d6) configuration agree with octahedral configuration [ref], table3.1. The conductance measurements in DMFexhibited that the complex has electrolytic nature indicate, therefore the two (Cl-) ions are located outside the coordination zone. Thus from the data above and those obtained from FT-IR spectra, flame atomic absorption also elemental analyses (C.H.N.S), the octahedral geometry around Pt(IV) ion can be suggested as shown in scheme 3.3:

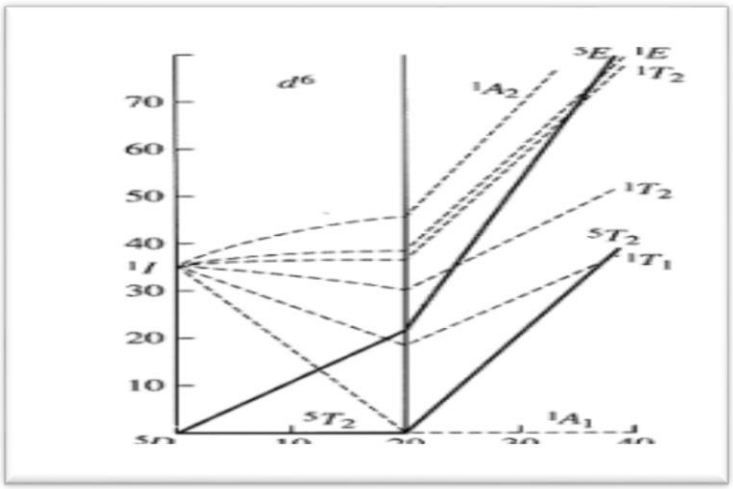

Scheme (3.2): Tanabe– Sugano energy diagram of d^6 in octahedral ligand field and suggested structure of L_2Pt complex

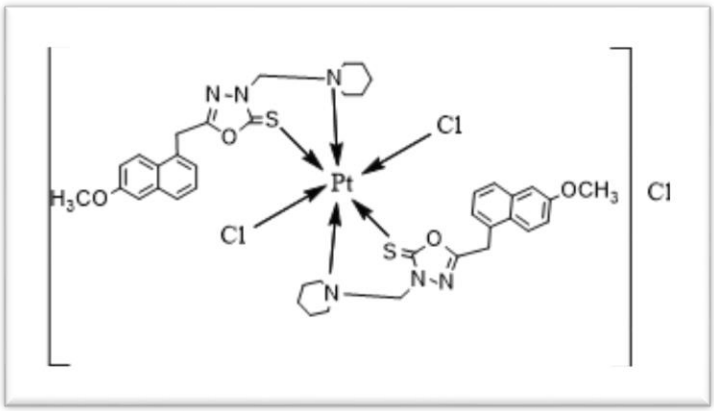

Scheme3.3 Geometry for L_2Pt

ISSN: 1343-4292
Volume 140, Issue 07, October, 2022

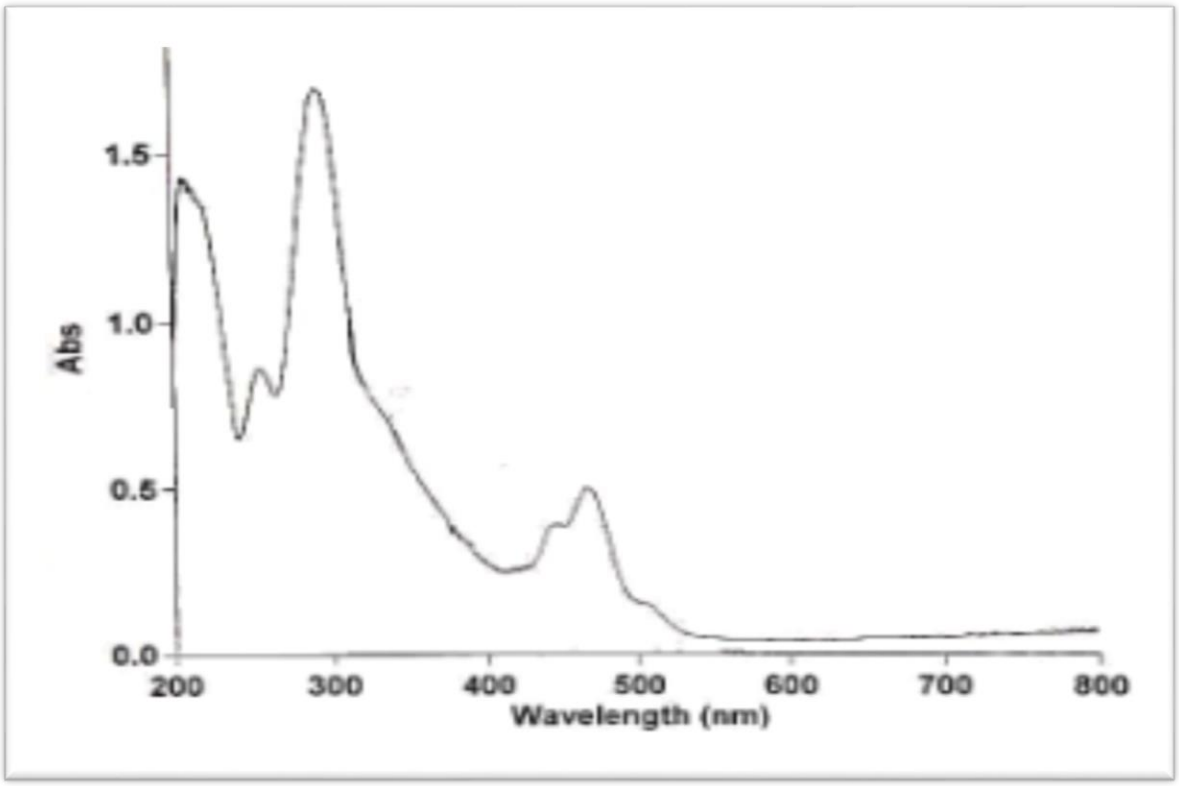

Fig 3.3 UV spectrum for Pt L

Table (3.1) Electronic spectral data of complexes

Symbol	Maximum absorption $\upsilon_{max}(cm^{-1})$	Band assignment	Suggested geometry
LCu	14492 23148,25063	$^2B_1g \rightarrow {}^2A_1g$ $^2B_1g \rightarrow {}^2B_2g + {}^2Eg$	**S.P**
LPt	19685 22831 30303	$^1A_1g \rightarrow {}^3T_1g$ $^1A_1g \rightarrow {}^3T_2g$ L→Pt(CT)	**O.h**

FT-IR spectra

The infrared spectra of the Mannich base or ligand shown in Fig3.4: showed bands at 3145 cm^{-1}, due to ν(NH) in the spectrum of oxadiazole and appear a new of bands in the region (2995 and 2837) cm^{-1} of the (νCH) attributed to the methylene group of (νCH2–N), [7] also the band at (1062,1078) and (1593) cm^{-1} respectively due to the stretching vibration of (νC=S) and (νC=N) respectively.

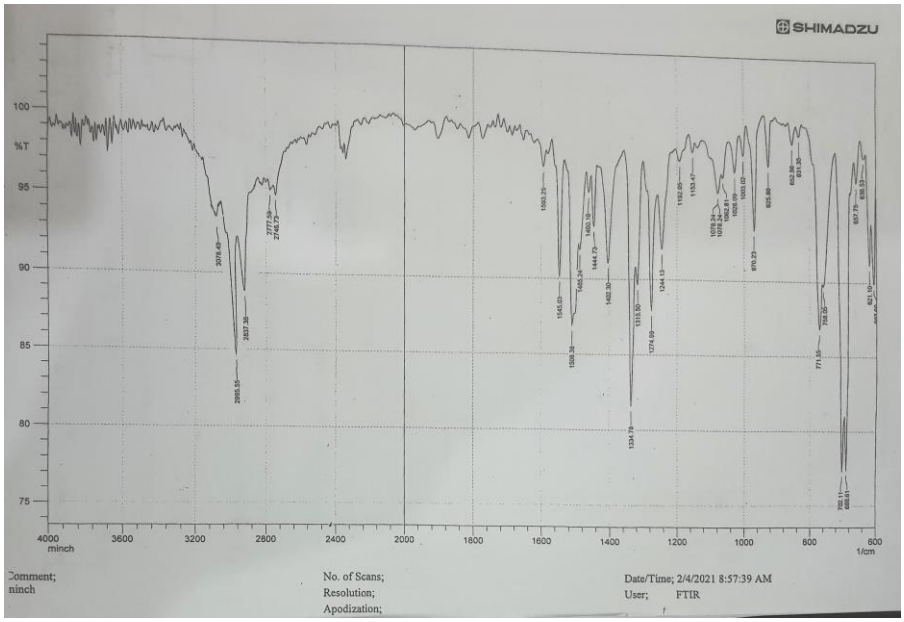

Fig 3.4 FT-IR spectrum for ligand

Infrared Spectra of Metal Complexes

The most significant changes between the IR spectra of the ligand and their metal complexes were;

A- The free ligand (L) showed three bands located at [(2995),(2837)],[(1078,1062)] and (1593) cm-1 corresponding to υ (CH2N), υ (C=S) groups and υ (C=N) for oxadiazole ring respectively [ref[. The ligand (L) behaved as a bidentate coordinating to metal ion through nitrogen of the (methylene group) and sulpher of thio carbonyl group these bands were shifted to a lower or higher frequencies.

B- In two complexes, the υ (C=S) and υ (CH2N) groups in the ligand (L) were shifted to higher frequencies or appeared as multiple bands with difference in its shape and reduced of intensity in spectra of prepared complexes[ref], this shift of frequency, change in form, and location for the stretching vibrations υ (C=S) thione group and υ (CH2N)given an evidence about the coordination of metal ion with (N) atom of (methylene group) group and (S) atom of thion group to make stable five membered chelate ring, [18]. The significant stretching vibrations of L and its complexes are listed in the table 3.2.

C- The spectra of (L) complexes showed new bands, which was not observed in spectrum of free ligand, these bands were located at range (516- 532), (400 - 428) and (380) cm-1 which was assigned to ν(M-N), ν(M-S) and (M-Cl) respectively [7].

Table (3.2): FTIR spectral data (cm-1) of (L)ligand and its metal complexes.

Comp.	υ (CH_2N)	***υC=N of oxadiazole ring***	***υC=S***	***υM-N***	***υM-S***	***υM-Cl***
L	2837,2995	1593	1062,1078	--------	------	--------
L Cu	2872,2939,2982	1593	1047,1072	532	428	--------
L Pt	2875,2939,2982	1595	1074	516	400	380

ISSN: 1343-4292
Volume 140, Issue 07, October, 2022

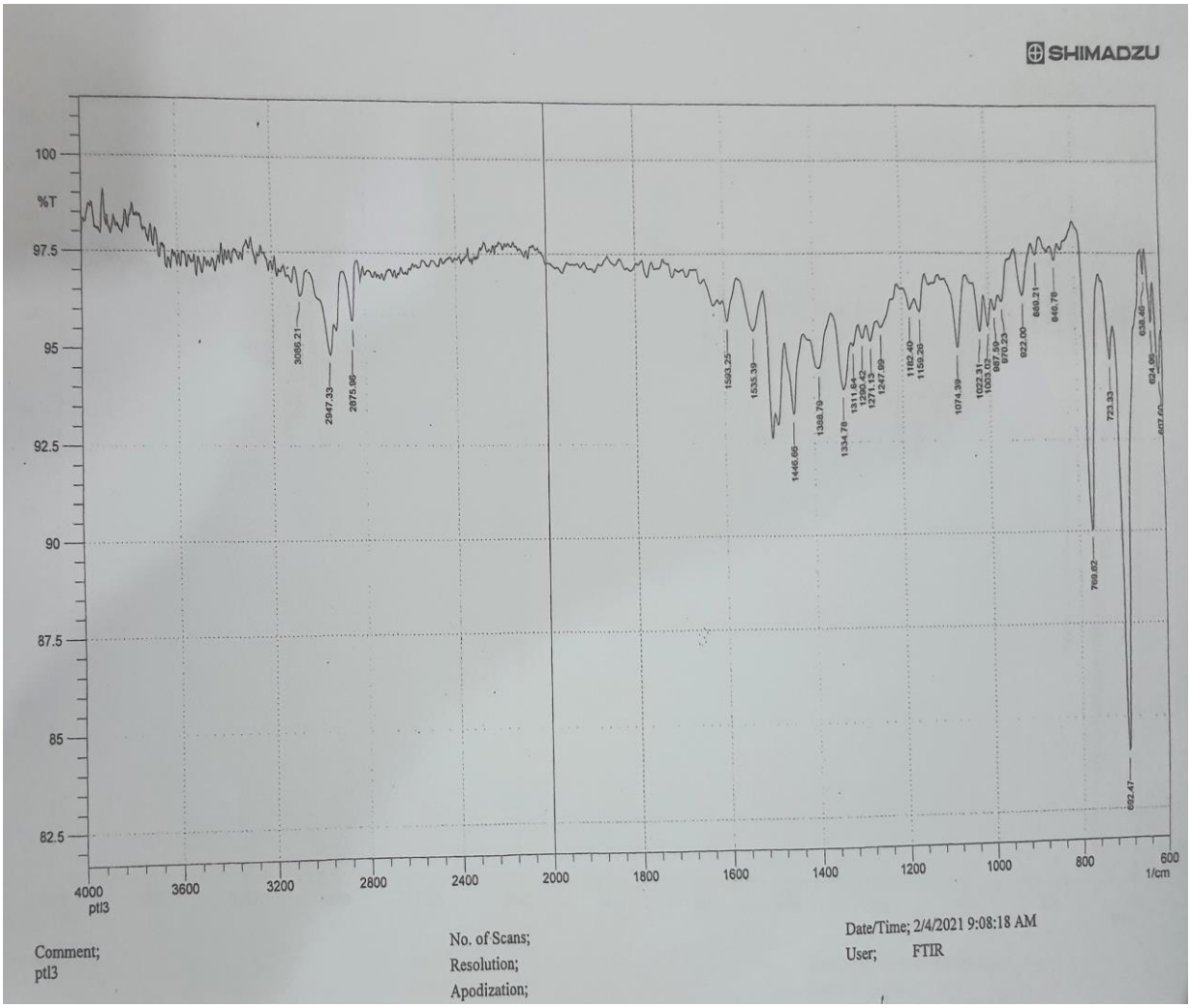

Figure 3.5 FT-IR for PtL

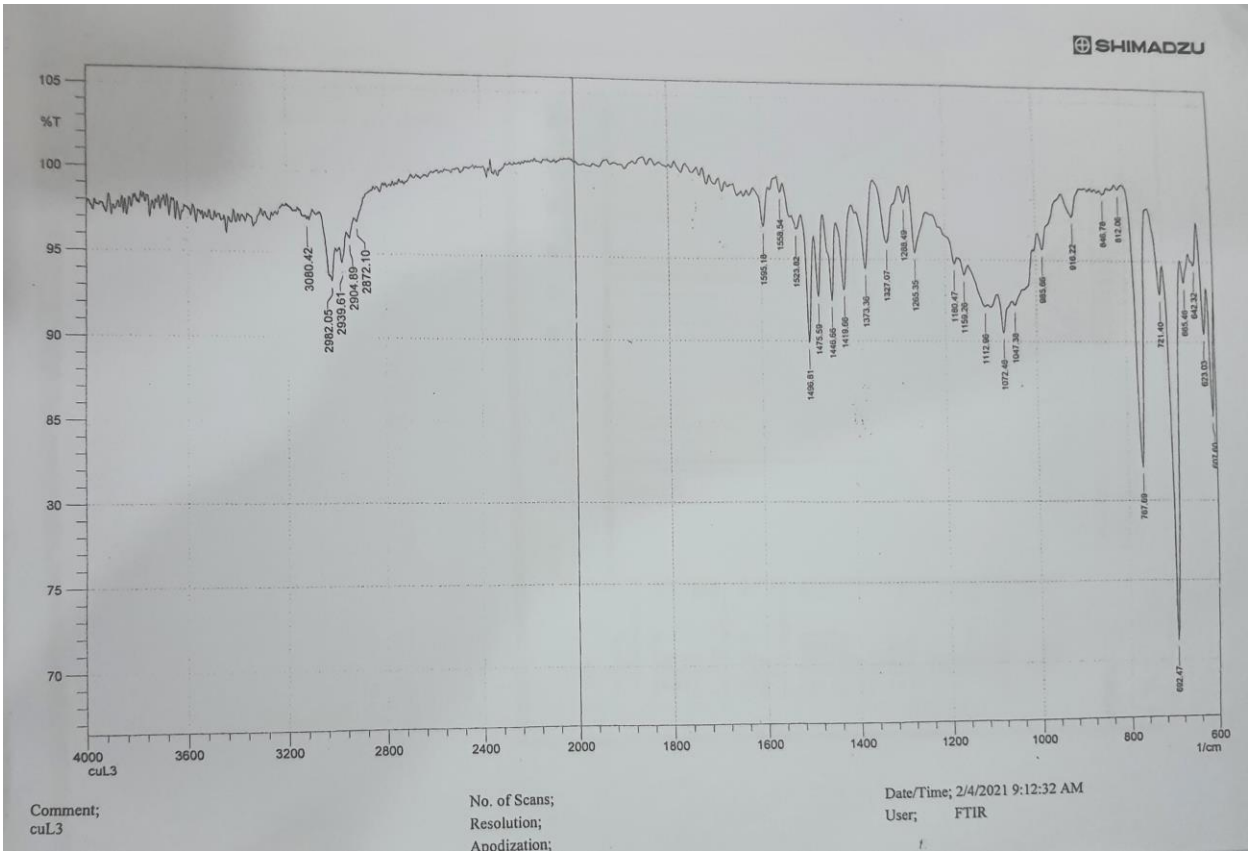

Figure 3.6 FT-IR for CuL

Elemental analysis

Elemental analysis CHNS and atomic flame absorption were shown in the below table with some physical properties for prepared compounds.

Table (3.3): Some analytical and physical data of (L) ligand and its complexes

Comp	Empirical formula	Mwt g.mol^{-1}	M.P C^0	Color	Element analysis % Experimental (theoretical)				
					C	H	N	S	M
(L)	$C_{20}N_3O_2SH_{23}$	369	150-152	White	65.22 (65.04)	5.98 (6.23)	11.42 (11.38)	9.03 (8.67)	
LCu	[Cu L Cl_2] H_2O $[Cu(C_{20}H_{23}N_3SO_2)Cl_2]$	503.5	Deco. 250	Dark green	48.04 (47.67)	4.79 (4.57)	8.52 (8.34)	6.68 (6.36)	13.12 (12.62)
LPt	$[Pt\ (L)_2Cl_2]\ Cl_2$ $[Pt\ (C_{40}H_{46}N_6S_2O_4)Cl_2]$ Cl_2	1151	Deco. 310	Dark reddish	46.12 (45.81)	4.67 (4.39)	8.94 (8.02)	6.49 (6.11)	19.04 (18.62)
				brown					

ISSN: 1343-4292
Volume 140, Issue 07, October, 2022

[1]H-NMR

The proton nuclear magnetic resonance spectra of the newly synthesized ligand (L), Fig.(3.7) in d^6DMSO solution with tetramethylsilan as an internal reference. The identification was done using simple splitting patterns that were produced by coupling of the protons which they have very different chemical shifts. According to the results obtained from the chemical shifts spectra, the molecular structure of the ligand (L) can be illustrated as shown in Table (3.4) [13].

The data of ^{13}C-NMR (L) displayed good solubility in DMSO, Fig(3.8). The carbon nuclear magnetic resonance spectral data gave additional support for the composition of the ligand (L). According to the results obtained from the chemical shifts spectra, the molecular structure of the ligand (L) can be illustrated as shown in Table (3.4) [17].

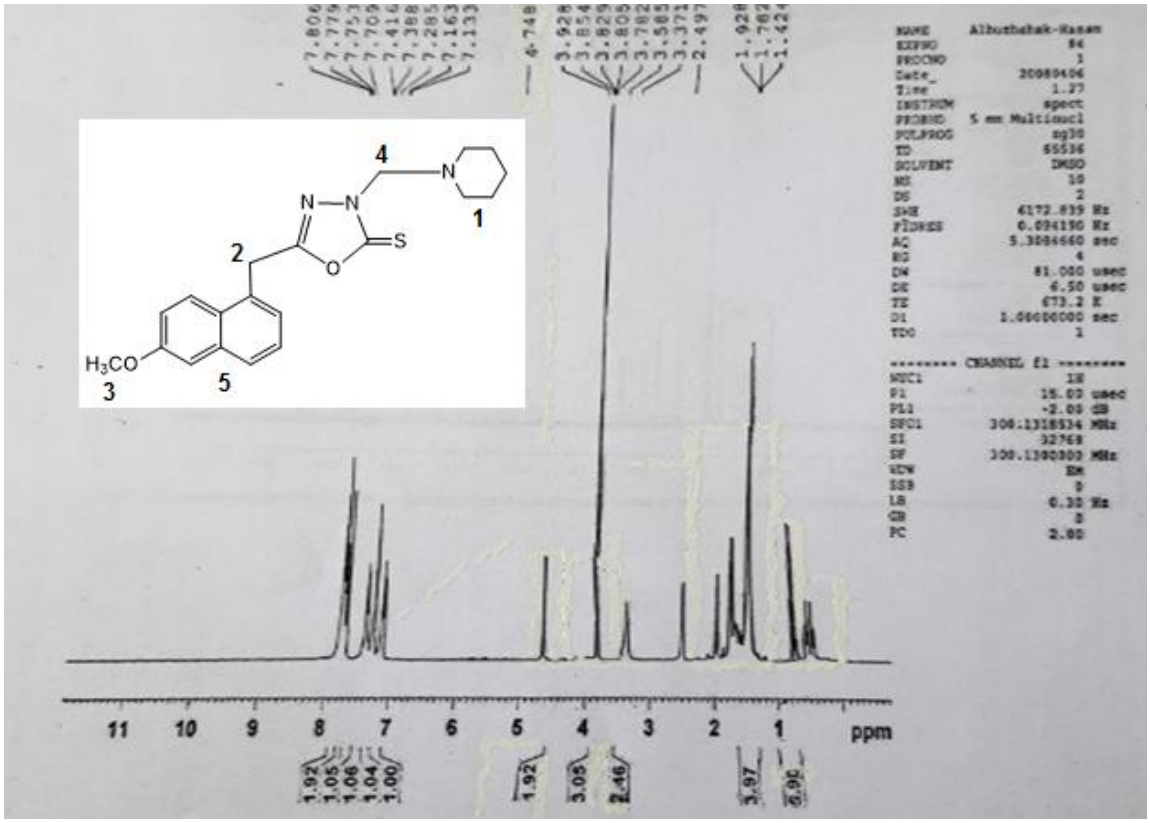

Figure 3.7 [1]H-NMR for ligand

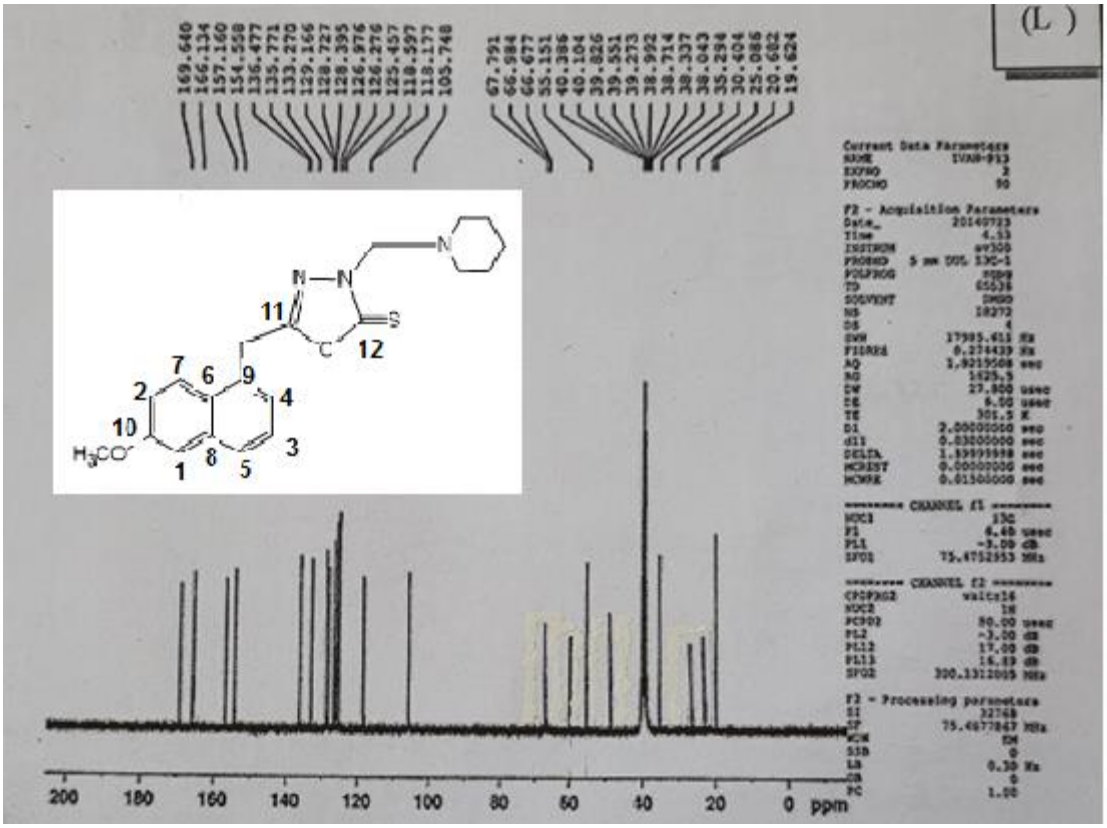

Figure 3.8 ^{13}C-NMR for ligand

Table 3.4: ^{1}H NMR and ^{13}C NMR spectral data, chemical shifts and assignments of (L)

Symbol	***Assignment ligand***	***Chemical shifts (ppm) (no. of protons and carbons)***
L	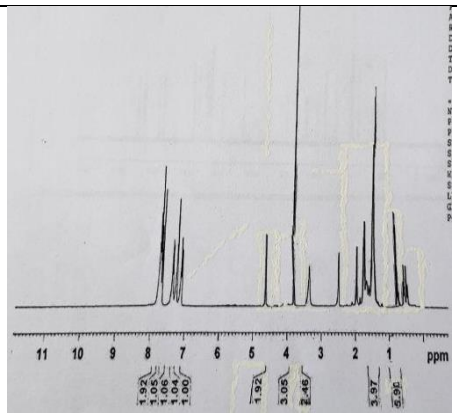	--multiple signals at 0.5-0.9 ppm, for CH_2 in pipyridine ring (C1) --singlet 3.86 ppm for two aliphatic protons CH_2 C2 -- singlet 3.87 ppm for three protons at OCH_3 -- singlet 4.8-4.9 ppm for two protons in CH_2 -- multiplet 7.13-7.8 ppm, for aromatic protons

ISSN: 1343-4292
Volume 140, Issue 07, October, 2022

L	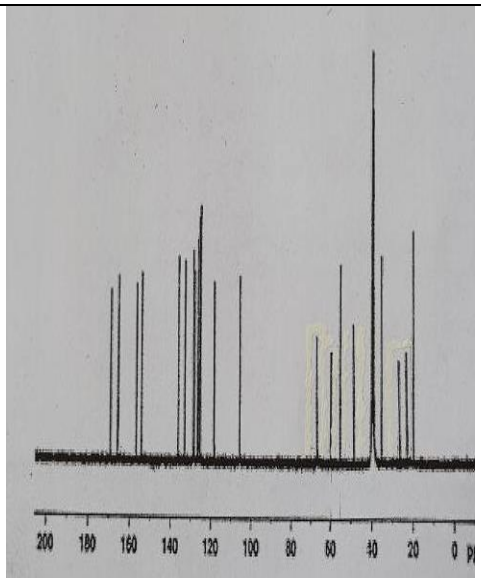	C of pipyridine 20,25.5,28,51 ppm CH_2 56 ppm OCH_3 60 ppm CH_2 Mannich 67.7 ppm C1 106 ppm, C2 118.5 ppm, C3 126.3 ppm C4 127 ppm, C5 128.4 ppm, C6 129ppm, C7 129.2 ppm, C8 135.7 ppm, C9 136.5 ppm C10 157.2 ppm, C11 166.2 ppm, C12 169.6 ppm

Molar Conductance and Magnetic Moment

The effective magnetic spin measurement of complexes was measured which listed in the table (3.5), these values have been corrected for the resulting magnetic effects [5], [14].

Table (3.5): Molar Conductance and Magnetic Moment of Metal Complexes

Complex Symbol	Complex Formula	Molar Cond. $S.cm^2.mol^{-1}$	µeff. B.M
LCu	$[Cu(L)\ Cl_2]$	11.56	1.82
LPt	$[Pt(L)_2]Cl_2]\ Cl_2$	169.22	0.05

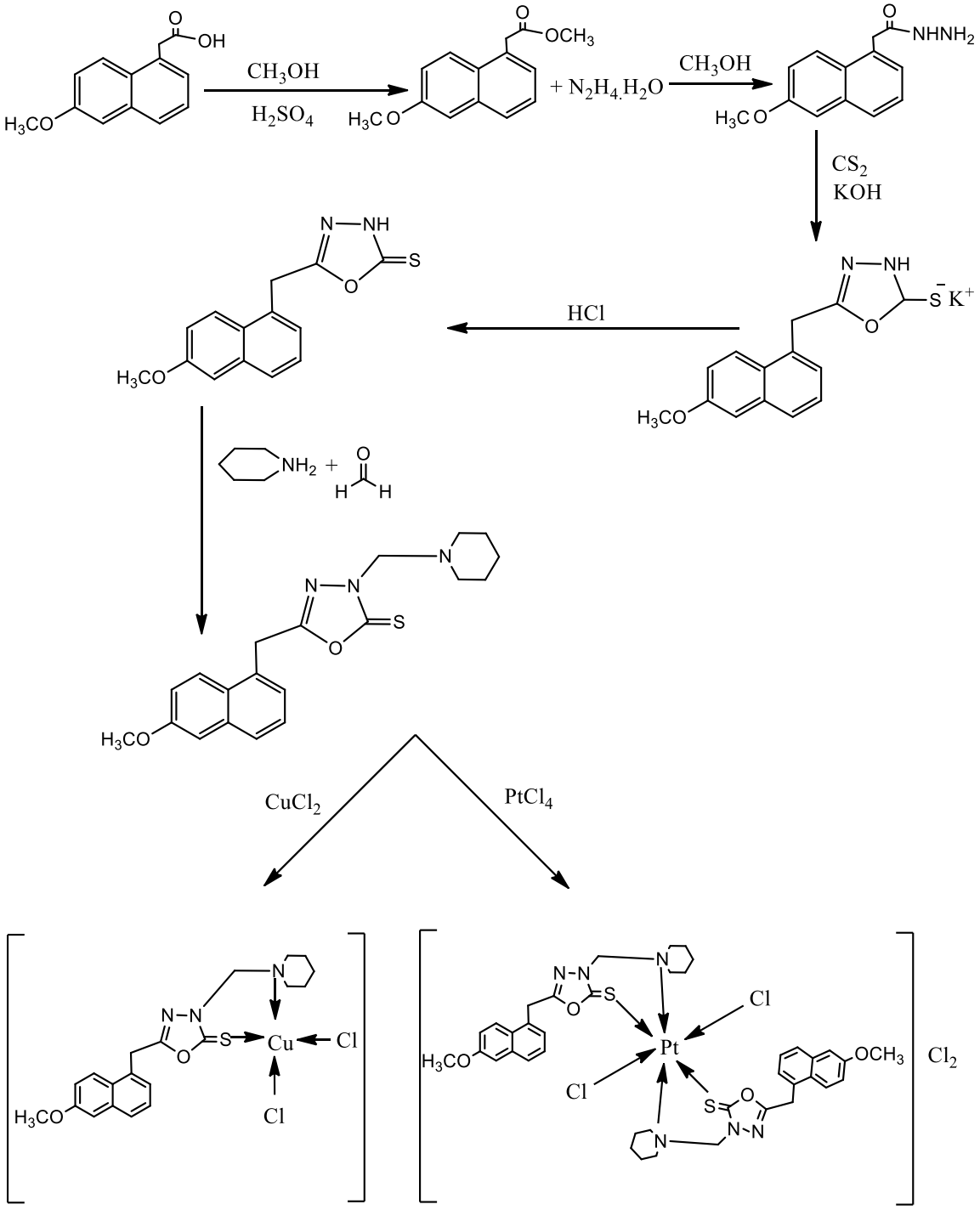

Scheme 3.4: flowchart for the synthesis of ligand and complexes.

Biological Activity

1. Antibacterial and Antifungal

Both of ligand and complexes give an clear inhibition effect against bacterium *Escherichia coli*(gram negative) and *Staphylococcus aurous* (gram positive) also against fungi *Candida albicans Aspergillus flavus* table3.6 . The results revealed that all tested complexes showed relatively higher activity against Gram - negative bacteria than that of Gram-positive bacteria. The Minimum Inhibition Concentration MIC for the complex is lesser than ligand as lesser than Amoxicillin and Ampicillin drugs, that indicates our compounds can act as antibacterial or anti fungi with little concentrations as shown in table 3.7.

ISSN: 1343-4292
Volume 140, Issue 07, October, 2022

Table 3.6: Antibacterial and antifungal activities for Manich (L) ligand and their metal complexes at (10^{-3} M)

Symb.	*Escherichia coli*	*Staphylococcus aurous*	*Candida albicans*	*Aspergillus flavus*
Control (DMSO)	-	-	-	-
(L)	4	2	35	30
Cu	10	8	19	22
Pt	18	12	19	23
Where :[6-8: (+),8-10: (++), >10: (+++)]			**Where :[30-40: (+++),20-30: (++++), 10-20: (+++++)]**	

Table 3.7: Minimal inhibitory concentration (MIC) for Manich (L) ligand and their metal complexes (µgm. ml^{-1})

Symb.	*Escherichia coli*					*Staphylococcus aurous*				
	0.025	0.05	0.075	0.1	0.5	0.025	0.05	0.075	0.1	0.5
(L_1)	+	+	(MIC)	-	-	+	+	+	(MIC)	-
Cu	+	(MIC)	-	-	-	+	+	(MIC)	-	-
Pt	(MIC)	-	-	-	-	(MIC)	-	-	-	-
Ampicillin	+	+	+	(MIC)	-	+	+	+	+	(MIC)
Amoxicillin	+	+	+	(MIC)	-	+	+	+	+	(MIC)

Where: (+): Growth, (MIC): 99%, (-): No growth

2. cytotoxicity result

Both complexes and ligand were tested *in vitro* for their cytotoxicity against normal cell(MDCK) using MTT assay procedure and also for determine their IC50 as shown in table 3.8 and figures 3.9, 3.10 and 3.11. the results showed that LD50 of L = 936 µg/ml, toxicity of Pt = 875 µg/ml and toxicity of Cu = 1356 µg/ml. Toxicity also tested for the ligand and both complexes against Human lung cancer cell line, the results showed that LD50 of Pt complex = 615 µg/ml, toxicity of Cu complex = 653 µg/ml and toxicity of free ligand = 620 µg/ml as shown in figures 3.12, 3.13 and 3.14 below.

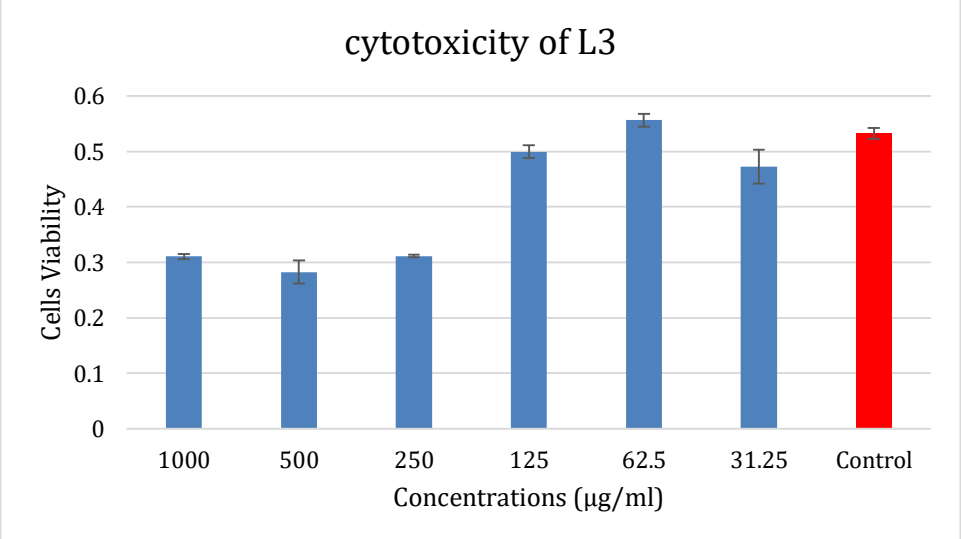

Fig 3.9: Cytotoxicity of Pt complex against MDCK cell line.

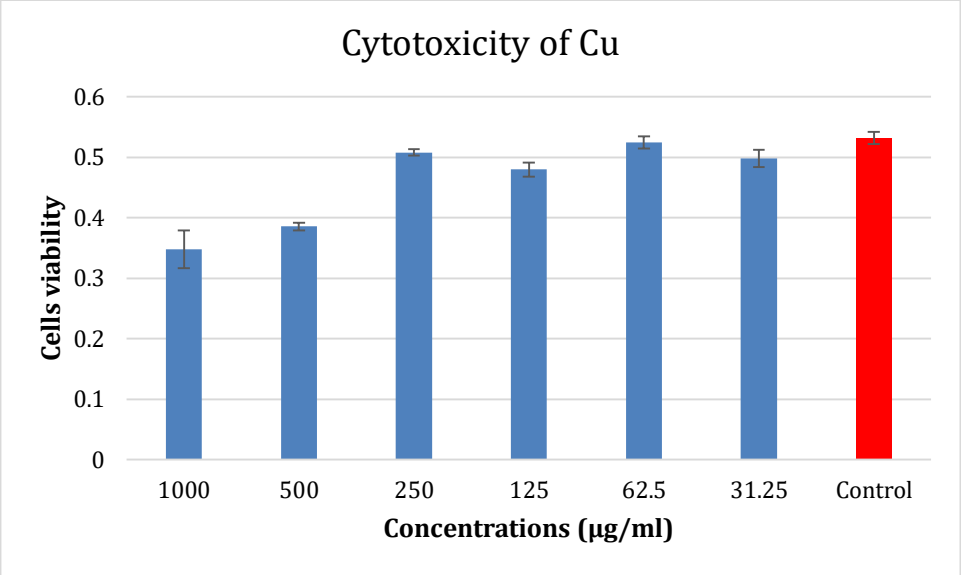

Fig 3.10: Cytotoxicity of Cu complex against MDCK cell line.

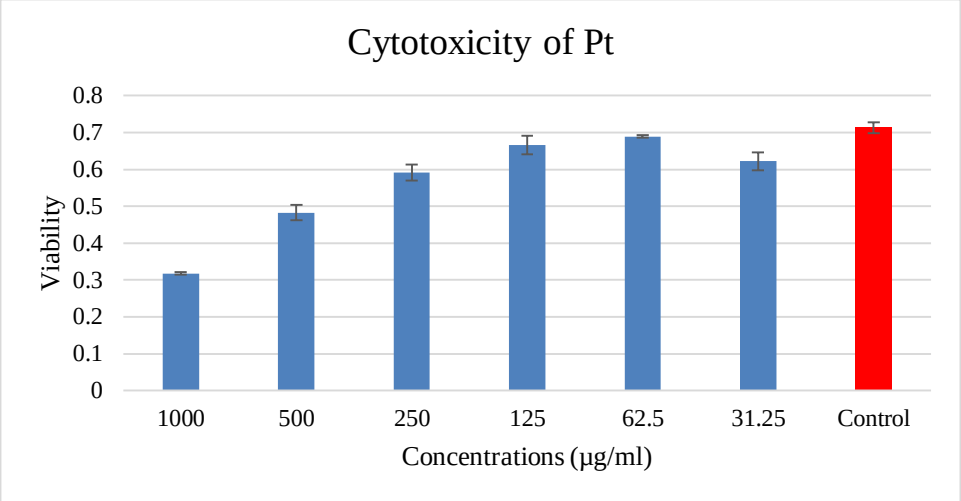

Fig 3.11: Cytotoxicity of Ligand against MDCK cell line.

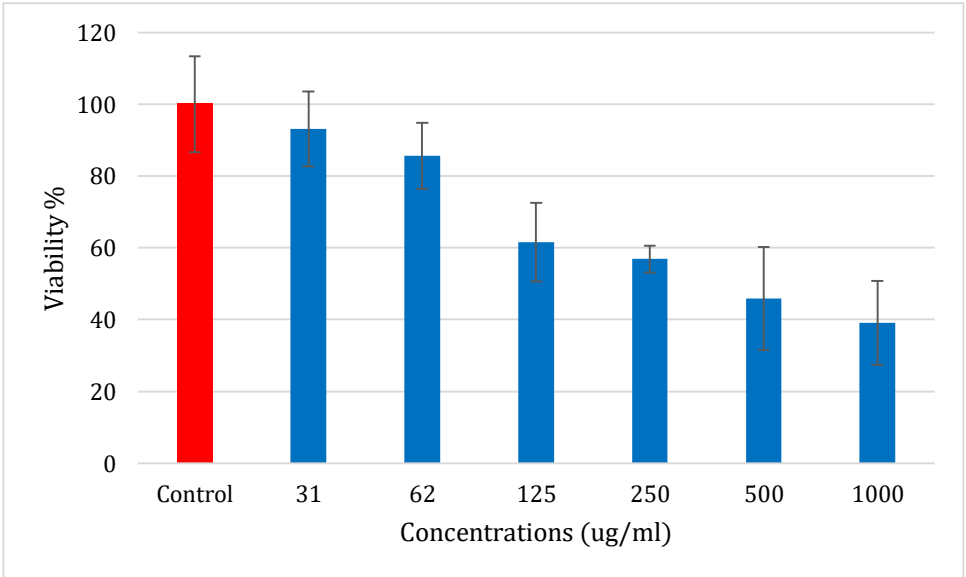

ISSN: 1343-4292
Volume 140, Issue 07, October, 2022

Fig 3.12: Cytotoxicity of Pt complexes against cancer cell line.

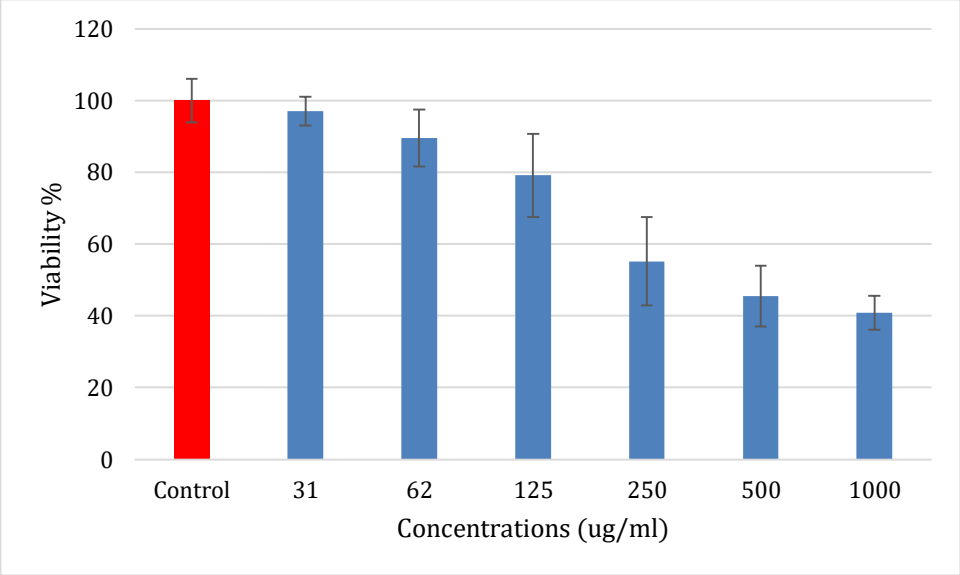

Fig 3.12: Cytotoxicity of Cu complexes against cancer cell line.

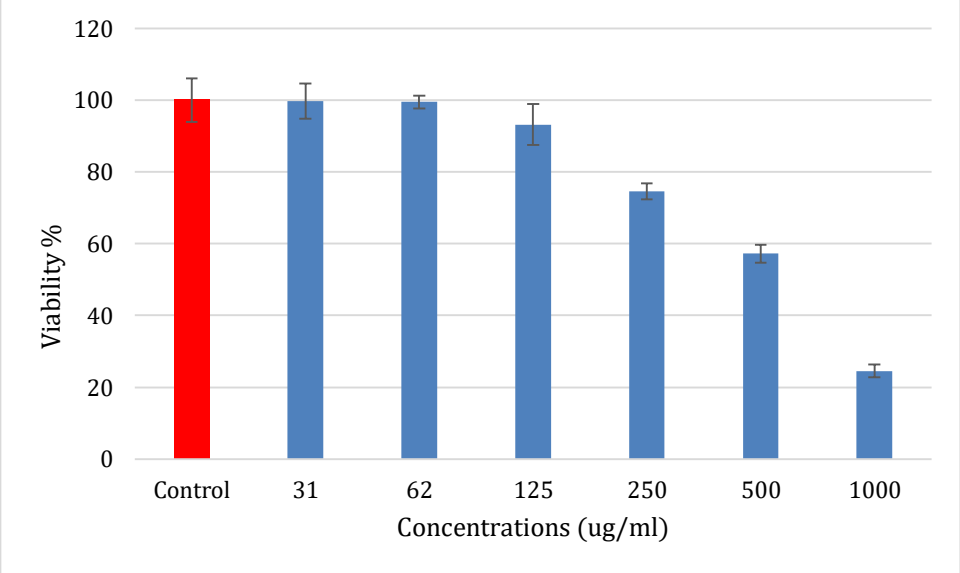

Fig 3.12: Cytotoxicity of free ligand against cancer cell line.

Hemolysis results

The result of hemolysis test revealed that hemolysis percentage of complexes solution approximately similar to percentage of control with relatively best result for cupper than platin complex.

solution	absorbance	H %
blank	0.996	
control	2.298	100
Pt complex	1.975	75.19
Cu complex	2.278	98.46

4. Conclusion

The spectroscopically confirmed structure for ligand was comlexed with salt of Pt(IV) and Cu(II), produced complexes were also approved their structure and properties by many techniques include UV, FT-IR, ^{1}H-NMR, ^{13}C-NMR, Molar conductivity and magnetic susceptibility and reveal that a ligand has bidentate chelating and coordinated with Pt as octahedral geometry complex and with Cu as square planer geometry complex. Biological activity was carry out against *Escherichia coli*(gram negative) and *Staphylococcus aurous* (gram positive) as antibacterial, against *Candida albicans and Aspergillus flavus* as antifungal and on normal cell MDCK cell line for test the cytotoxicity. The result approve for the complexes may be work as antibacterial and antifungal. From the cytotoxicity test our compounds can be consider as drug, table 4.1.

Table 4.1 Inhibition concentrations and IC50 values of ligand and complexes.

Conc. µg/ml	L3		Cu L		Pt L	
	availability	inhibition	availability	inhibition	availability	inhibition
1000	58.34	41.66	65.38	34.62	44.41	55.59
500	53.08	46.92	72.48	27.52	67.47	32.53
250	58.53	41.47	95.44	4.56	82.63	17.37
125	93.85	6.15	90.14	9.86	93.05	6.95
62.5	104.51	Reactivation	98.59	1.41	96.30	3.70
31.25	88.77	11.23	93.61	6.39	87.00	13.00
IC50	936 µg/ml		1365 µg/ml		875 µg/ml	

5. References

[1] Akram, M. et al. (2018) 'Synthesis, biological evaluation and molecular docking studies of mannich bases derived from 1, 3, 4-oxadiazole-2-thiones as potential urease inhibitors', Tropical Journal of Pharmaceutical Research, 17(1), pp. 127–134. doi: 10.4314/tjpr.v17i1.18.

[2] Al-Hasani, R. A. M. (2008) 'Mannich Base Derived From 1,3,4-Thiadiazole As Chelating Ligand for Some Transition Metal Complexes', Journal of Al-Nahrain University Science, 11(2), pp. 42–56. doi: 10.22401/jnus.11.2.06.

[3] Al-Jeboori, M. J., Abdul-Ghani, A. J. and Al-Karawi, A. J. (2008) 'Synthesis and structural studies of new Mannich base ligands and their metal complexes', Transition Metal Chemistry, 33(7), pp. 925–930. doi: 10.1007/s11243-008-9134-3.

[4] Bala, S. et al. (2014) 'Mannich Bases: An Important Pharmacophore in Present Scenario', International Journal of Medicinal Chemistry, 2014(Figure 1), pp. 1–15. doi: 10.1155/2014/191072.

[5] Bayoumi, H. H., Alaghaz, A. N. and Aljahdali, M. S. (2013) 'Cu(II), Ni(II), Co(II) and Cr(III) complexes with N2O2-chelating schiff's base ligand incorporating azo and sulfonamide moieties: Spectroscopic, electrochemical behavior and thermal decomposition studies', International Journal of Electrochemical Science, 8(7), pp. 9399–9413.

[6] Ganot, N. et al. (2013) 'Anticancer metal complexes: synthesis and cytotoxicity evaluation by the MTT assay.', Journal of visualized experiments : JoVE, (81), pp. 1–6. doi: 10.3791/50767.

[7] Ganzoury, M. A. et al. (2015) 'Introduction to Fourier Transform Infrared Spectrometry', Renewable

and Sustainable Energy Reviews, 50, pp. 1–8. doi: 10.1016/j.rser.2015.05.073.

[8] Hussain, A. et al. (2019) 'Copper(II) complexes as potential anticancer and Nonsteroidal anti-inflammatory agents: In vitro and in vivo studies', Scientific Reports. Springer US, 9(1), pp. 1–17. doi: 10.1038/s41598-019-41063-x.

[9] Krishnan, S., Ridhar, S. and Amesh, A. R. (2001) 'Synthesis and Pharmacological Activities of Hydrazones , Schiff and Mannich Bases of Isatin Derivatives', 24(October), pp. 1–4.

[10] Mohammadizadeh, F. et al. (2018) 'The cytotoxicity effects of a novel Cu complex on MCF-7 human breast cancerous cells', BioMetals. Springer Netherlands, 31(2), pp. 233–242. doi: 10.1007/s10534-018-0079-5.

[11] Muhannad A . Mahmood, R. M. . D., Jassim, W. K. . and Aday, S. T. (2012) 'Synthesis and characterization of some New Mannich bases and their thione derivatives .', Kerbala journal of pharmaceutical sciences, 2(3), pp. 223–233.

[12] Neelakantan, M. A. et al. (2018) 'Interaction of Amino Acid Schiff Base Metal Complexes with DNA/BSA Protein and Antibacterial Activity: Spectral Studies, DFT Calculations and Molecular Docking Simulations', Applied Organometallic Chemistry, 32(4), pp. 1–19. doi: 10.1002/aoc.4259.

[13] Rakowski, M. C., Rycheck, M. and Busch, D. H. (1975) 'Synthesis and Characterization of Transition Metal Complexes Containing a Pentadentate Macrocyclic Ligand', Inorganic Chemistry, 14(5), pp. 1194–1200. doi: 10.1021/ic50147a045.

[14] Rauen, A., Soffel, H. C. and Winter, H. (2000) 'Statistical analysis and origin of the magnetic susceptibility of drill cuttings from the 9.1-km-deep KTB drill hole', Geophysical Journal International, 142(1), pp. 83–94. doi: 10.1046/j.1365-246X.2000.00141.x.

[15] Roman, G. et al. (2007) 'Synthesis of new Mannich Bases derived from 5-phenyl-1,3,4-oxadiazole-2-thione and investigation of the conformational isomers of dimethyl 5-(5-phenyl-2-thioxo-1,3,4-oxadiazole-3-methylamino)isophthalate', Revue Roumaine de Chimie, 52(12), pp. 1103–1110. doi: 10.1002/chin.200901136.

[16] Sathish Kumar, K. et al. (2013) 'Synthesis, Characterization, and Biological and Cytotoxic Studies of Copper(II), Nickel(II), and Zinc(II) Binary Complexes of 3-Amino-5-methyl Isoxazole Schiff Base', ISRN Inorganic Chemistry, 2013, pp. 1–7. doi: 10.1155/2013/562082.

[17] Silva, H. et al. (2010) 'Synthesis, characterization, and cytotoxic activity of novel platinum(II) complexes derived from n-benzyl-ethylenediamine and oxalate: Research letter', Chemical Biology and Drug Design, 75(4), pp. 407–411. doi: 10.1111/j.1747-0285.2009.00941.x.

[18] Al Zoubi, W. et al. (2018) 'Synthesis, characterization, and biological activity of Schiff bases metal complexes', Journal of Physical Organic Chemistry, 31(2), pp. 1–7. doi: 10.1002/poc.3752.

This work is licensed under a Creative Commons Attribution Non-Commercial 4.0 International License.